HUMAN BIOLOGY
2024, VOL. 94, ISSUE 5
ORIGINAL ARTICLE

OPEN ACCESS

Hsa_circ_0000038 Inhibits the Progression of Hepatocellular Carcinoma by Sponging miR-92a-2-5p to Regulate the p53/p21 Pathway

Si-hang Zhang[1,2], Meng-ting Luo[2], Zheng-yuan Zeng[2,3], Xingtong Li[2], Renchao Zou[4], QianFeng[5], Tai-Cheng Zhou[2], Jia Wei[2*]*

ABSTRACT

Background: The diagnostic potential of circular RNAs (circRNAs) has garnered significant attention recently. However, the specific mechanisms by which various circRNAs operate in different cancers, particularly hepatocellular carcinoma (HCC), require further investigation.

Methods: Quantitative real-time fluorescence polymerase chain reaction (RT-qPCR) was utilized to evaluate the expression levels of hsa_circ_0000038. Western blotting was employed to assess the protein expression levels of p53, p21, and p27. To comprehensively understand the functional implications of hsa_circ_0000038, a series of cellular assays were performed, including cell clonal formation experiment, the CP6 system for cell proliferation and Transwell assays for evaluating invasion and migration. Additionally, luciferase and co-immunoprecipitation assays were conducted to explore the interactions between miR-92a-2-5p and hsa_circ_0000038 or Tp53.

Results: Our findings demonstrated that hsa_circ_0000038 was significantly downregulated in both HCC tissues and cell lines. Overexpression of hsa_circ_0000038 was shown to arrest the cell cycle of HepG2 cells (p53 wild-type) at the G0–G1 phase, thereby repressing cell proliferation, invasion, and migration in vitro. In contrast, hsa_circ_0000038 overexpression had minimal effects on the cell cycle in Hep3B cells (p53-deficient). Co-transfection with miR-92a-2-5p partially mitigated the effects of hsa_circ_0000038 in HepG2 cells. Further analysis revealed that hsa_circ_0000038 directly binds to miR-92a-2-5p and that Tp53 mRNA is a direct target of miR-92a-2-5p. Through regulatory network analysis, hsa_circ_0000038 was shown to upregulate the expression of p53, p21, and p27 proteins.

Conclusion: This study highlights the downregulated expression of hsa_circ_0000038 HCC and identifies it as a crucial regulator of the miR-92a-2-5p/p53/p21 axis. These findings suggest that hsa_circ_0000038 may play a significant role in inhibiting HCC progression through cell cycle arrest. Furthermore, this research enhances our understanding of the complex molecular mechanisms underlying hepatocarcinoma pathogenesis.

INTRODUCTION

Hepatocellular carcinoma (HCC) is the most common type of primary liver cancer and ranks as the third leading cause of cancer-related mortality worldwide Sung et al. (2021), Llovet et al. (2021). Current diagnostic methods, both invasive and non-invasive, are primarily effective during the middle to late stages of HCC Ayuso et al. (2018), Yang et al. (2019). Unfortunately, the sensitivity and specificity of existing tumor biomarkers are often inadequate. Despite advancements in treatment strategies Sugawara et al. (2021), Reig et al. (2022), Singal et al. (2023), the prognosis for HCC patients remains poor, primarily due to the lack of timely early diagnosis Huang et al. (2020). Therefore, there is an urgent need for identification and validation of novel molecular biomarkers to improve early detection, prognosis, and treatment outcomes for HCC patients. Circular RNAs (circRNAs) plays a pivotal role in a variety of malignancies, including HCC Yao et al. (2017). Their impact on tumorigenesis is twofold; they can act as either tumor suppressors or proto-oncogenes, regulating tumor growth and progression. Due to their lack of 5'-3' polarity and polyadenine tails,

[1]Kunming Medical University, Kunming, Yunnan Province, China.
[2]Central Lab, The Affiliated Hospital of Yunnan University, Kunming, Yunnan Province, China.
[3]Yunnan University, Kunming, Yunnan Province, China.
[4]Department of Hepatobiliary Surgery, The Second Affiliated Hospital of Kunming Medical University, Kunming, 650101, Yunnan, China.
[5]Department of Clinical Laboratory, Affiliated Hospital of Yunnan University.
Correspondence to: Dr. Jia Wei, The Central Laboratory of the Affiliated Hospital of Yunnan University, Kunming 650203, Yunnan, China. E-mail: weijia19631225@163.com.
Tai-Cheng Zhou, The Central Laboratory of the Affiliated Hospital of Yunnan University, Kunming 650203, Yunnan, China. E-mail: zhoutc@ynshhyy.com.
Keywords: hsa_circ_0000038; HCC; miR-92a-2-5p; cell cycle

circRNAs are more resistant to RNase degradation compared to their linear counterparts, making them more suitable as molecular markers than mRNA. One study indicated that hsa_circ_0000038 may be a differential downregulated circRNA in colorectal cancer Mohammadi et al. (2022). Our findings also show that hsa_circ_0000038 is down-regulated in HCC tissues. However, the mechanism by which hsa_circ_0000038 functions in HCC requires further investigation. CircRNAs exert their effects by regulating the levels of miRNAs and target mRNAs through the competitive endogenous RNA (ceRNA) mechanism. We predicted that miR-92a may be a direct binding target of hsa_circ_0000038 and found that hsa_circ_0000038 could suppress HCC via the miR-92a/p53 pathway.

miR-92a, a well-studied microRNA, is recognized for its role in inflammatory and cancer diseases. Several studies have linked miR-92 to the promotion of cancer genes expression and its engagement in multiple classical cancer-associated pathways Xiong et al. (2018). Specifically, MiR-92a has been shown to facilitate hepatocellular carcinoma cell proliferation and invasion by targeting Recombinant Forehead Box Protein A2 (FOXA2) Wang et al. (2017). Moreover, miR92a-3p regulates the phosphatase and tensin homolog deleted on chromosome ten/ protein kinase B (PTEN/AKT) pathway in HCC Gong et al. (2018).

The susceptibility of tumor protein p53 (Tp53) to inactivation in hepatocellular carcinoma (HCC) underscores its critical role in the development and progression of this disease Ueda et al. (1995). Numerous studies have highlighted the association between p53 and various characteristics of HCC, including tumor differentiation, vascular invasion, and disease staging Muller et al. (2006). As key regulators of cell cycle arrest, both p53 and its downstream effector p21 play essential roles in orchestrating cellular responses. Specifically, p53 induces cell cycle arrest and apoptosis at the G1/S checkpoint primarily through the transcriptional upregulation of cyclin-dependent kinase (CDK) inhibitors p21 and PUMA/NOXA Lieschke et al. (2019). Furthermore, the activation of p53 can be modulated by circular RNAs (circRNAs), which display differential expression patterns in response to p53 activation Fischer et al. (2017), Du et al. (2017).

Our groundbreaking discovery identifies hsa_circ_0000038 as a negative regulator of the miR92a-2-5p, which, in turn, modulates the p53/p21 proteins to suppress tumor progression in HCC. These findings shed light on a novel molecular mechanism involving circRNA-mediated regulation of the p53 pathway and competing endogenous RNA (ceRNA) in HCC, contributing to a deeper understanding of HCC pathogenesis.

MATERIALS AND METHODS

Clinical specimens and HCC tissue collection

The research was approved by the Ethics Committee of the Affiliated Hospital of Yunnan University, Kunming, China. All subjects signed written informed consent. The inclusion criteria for patients were: Sung et al. (2021) clinical diagnosis of primary liver cancer, and Llovet et al. (2021) no prior treatment with antitumor drugs, radiotherapy, or chemotherapy. The exclusion criteria were: Sung et al. (2021) chronic hepatitis virus infection, Llovet et al. (2021) cirrhosis decompensation, Ayuso et al. (2018) serious organ lesions or cardiopulmonary insufficiency, Yang et al. (2019) HIV co-infection, Sugawara et al. (2021) progression to chronic hepatitis B-associated liver cancer or other tumors, Reig et al. (2022) severe anemia or malnutrition, and Singal et al. (2023) abnormal platelet and coagulation function. Fresh blood and tissue samples (20 pairs of HCC tissues and adjacent non-tumor tissues) were collected from patients. Blood samples were centrifuged at 3300 rpm for 5 minutes to obtain serum samples. All samples were frozen in liquid nitrogen and stored at −80°C until use.

Cell culture

Human HCC cell lines (HepG2 and Hep3B) were purchased from the Chinese Academy of Sciences (Kunming Institute of Zoology, CAS, China). The human hepatic progenitor cell line (HepaRG) was donated by the Department of Hepatobiliary Surgery, Second Affiliated Hospital of Kunming Medical University, Kunming, China. HepG2 cells are p53 wild-type, while Hep3B cells are p53-deficient. All cells were cultured in DMEM (Gibco, Grand Island, NY, USA) containing 10% inactivated fetal bovine serum (FBS, Gibco), 100 U/mL streptomycin, and 100 U/mL penicillin, in a moist incubator at 37°C and 5% CO2. Assays were conducted during the logarithmic growth phase of the cells.

RNase R assay

Total RNA was extracted from HepG2 cells. The RNA was divided into two parts: one treated with RNase R (RNase R+) and the other not treated (RNase R-). The reaction condition was 37°C for 20 minutes. The RNA was then purified and recovered for agar-gel electrophoresis.

RNA isolation and quantitative real-time PCR (RT-qPCR)

TRIzol reagent (Invitrogen, USA) was used to extract total RNA from cells, tissues, and plasma samples. RNA concentration was measured and stored at −80°C for future analysis. Real-time PCR was performed using an ABI12k

Fast Real-Time PCR System (Applied Biosystems, USA) with FastStart Universal SYBR Green Master (ROX) (Roche, Switzerland). Each sample had three replicates. The relative expression was calculated using the 2−ΔΔCt method. The PCR cycle included initial denaturation for 5 minutes at 95°C, followed by 40 cycles at 95°C for 15 seconds, and 1 minute of annealing/extension at 60°C. β-actin was used to normalize mRNA expression levels. Table1 lists the PCR primers.

Plasmid construction and cell transfection

The full-length sequence of hsa_circ_0000038 was amplified and chemically synthesized by PCR. Gene Seed (Guangzhou, China) inserted these segments into the pLC5-ciR vector, which includes artificial flanking sequences and splice acceptor/donor sequences. An antisense oligonucleotide (ASO) for hsa_circ_0000038 knockdown was constructed to target its back-splice sequence by Yaoyuan Biotechnology Company (Shanghai, China). Cells at 50–60% confluence were transfected with plasmids and ASO using Lipofectamine™ 3000 Transfection Reagent (Invitrogen, Shanghai, China). Table 2 showed details about other sequences.

Actinomycin D treatment

The cells were cultured and divided into two groups according to the experimental design.

HepG2 cells in each group were treated with actinomycin D (2 μg/ml) for 0, 12, and 24 h. At each time point, cells were collected, and the total RNA was extracted. Genomic DNA was removed using the PrimeScript RT Reagent Kit with gDNA eraser (Takara, Tokyo, Japan) and cDNA was synthesized by reverse transcription. RT-qPCR was performed using FastStart Universal SYBR Green Master (ROX) to detect the levels of target RNA and reference RNA.

Cell proliferation assay

Based on specific transfection, cell suspensions (5×10^3 cells/well) were inoculated into 96-well plates and pre-cultured for 24 hours. Absorbance was measured using the CP6 system (Applied Biophysics, USA). Measurements were taken over 96 hours after the cells had attached. In CCK8 assays, 10 μL of CCK8 solution was added to each well and incubated for 2.5 hours protected from light. Absorbance was measured at 450 nm and 650 nm using a Varioskan Flash system (Thermo, USA). Time points were 0h, 24h, 48h, and 72h after cell attachment.

In vitro invasion assay

Matrigel matrix (Corning, USA) was mixed 1:4 with FBS-free medium at 4°C and coated onto the upper chamber of the Transwell insert. Plates were incubated for 2 hours at 37°C to coagulate the gel, then 500 μL DMEM with 5% FBS was added to the lower chamber.

Table 1: Correlated primer sequence

Gene	primer (5'-3')
hsa_circ_0000038-qp	ATGACACCTACCTCAGTCATTCC
	TTGCTTGGGACAGTTCAGTCTGAT
hsa_circ_0000284-qp	GTCGGCCAGTCATGTATCAA
	ACCAAGACTTGTGAGGCCAT
hsa_circ_0000038 Divergent	AGTGTCTACGGGAGGAAGAAGA
	ATTGGTAGTAGTTCCGAGCCC
hsa_circ_0000038 convergent	CTGAACTGTCCCAAGCAATAAAC
	TCTGATAGCTTTCATCTTCATCTTC
Tp53	CAGCACATGACGGAGGTTGT
	TCATCCAAATACTCCACACGC
β-actin	GCACAGAGCCTCGCCTT
	GTTGTCGACGACGAGCG
U6	AGCACATATACTAAAATTGGAACGAT
	ACTGCAGGGTCCGAGGTATT
U6-RT	GTCGTATCGACTGCAGGGTCCGAGGTATTCGCAGTCGATACGACAAATATG
miR-92a-2-5p	GCGGGTGGGGATTTGTTG
	ACTGCAGGGTCCGAGGTATT
miR-92a-2-5p-RT	GTCGTATCGACTGCAGGGTCCGAGGTATTCGCAGTCGATACGACAAATATG

Table2: Correlated nucleotide sequence.

Gene	sequence (5'-3')
has-miR-92a-2-5p mimics	GGGUGGGGAUUUGUUGCAUUAC
has-miR-92a-2-5p inhibitor	GUAAUGCAACAAAUCCCCACCC
miR-NC mimics	UUGUACUACACAAAGUACUG
miR-NC inhibitor	CAGUACUUUUGUGUAGUACAA

The upper chamber was placed into 24-well plates. Transfected cells in the logarithmic growth phase were rinsed with PBS and suspended in serum-free DMEM. The concentration was adjusted to 1×10^5/mL and 150 μL was added to the upper chamber. After 48 hours, the upper chamber was fixed with 4% paraformaldehyde for 20–30 minutes, then stained with 0.5% crystal violet for 10 minutes. Invaded cells were counted under a light microscope in at least five random fields.

Western blotting

Protein was extracted from transfected cells using RIPA buffer, and concentration was determined using a BCA kit (Beyotime, Shanghai, China). Forty nanograms of protein were separated by electrophoresis on a 10% polyacrylamide gel and transferred to PVDF membranes (Millipore, Billerica, MA, USA). The membrane was blocked for 4 hours at room temperature, then incubated overnight at 4°C with primary antibodies: CDK4, CDK2 (1:5000, Proteintech, Beijing, China), p53 (1:1000, Proteintech), p21 (1:1000, Proteintech), cyclinD1, cyclinE1 (1:2500, Proteintech, Beijing, China), and β-actin (1:2000, Proteintech).

A horseradish peroxidase-conjugated secondary antibody was added. Images were captured using ChemiDoc XRS+ (Bio-rad, USA), and protein expression levels were analyzed with ImageJ software.

Dual-luciferase reporter assay

According to starBase v2.0 prediction, the binding site of hsa_circ_0000038 to miR-92a-2-5p was mutated by segmentation. miR-92a-2-5p may have two separate binding sites, so two mutants of hsa_circ_0000038 (part1 and part2) were constructed.

The wild-type and mutant hsa_circ_0000038 or wild-type and mutant Tp53 3'UTRs were inserted into the pmirGLO dual-luciferase vector (Beijing Tsingke Biotech Co., Ltd.). HEK-293T cells (5×10^4 cells/mL) in 96-well plates were co-transfected with the vectors (miR92a-2-5p mimics/NC and hsa_circ_0000038 wild/mut, miR92a-2-5p mimics/NC, and Tp53 wild/mut). Luciferase signals were read 24 hours post-transfection using a Dual-Luciferase Reporter Assay System (Promega, USA).

RNA immunoprecipitation assay

The RNA immunoprecipitation (RIP) assay was performed using an RNA immunoprecipitation kit (Geneseed, China) with AGO2-specific antibodies (Cat No. 67934-1-Ig, Proteintech) following the manufacturer's instructions. The immunoprecipitated RNAs were detected by RT-qPCR to measure levels of hsa_circ_0000038 and Tp53. A mouse isotype antibody (IgG) was used as the control.

Colony formation assay

Transfected HCC cells were plated into six-well plates and incubated under 5% CO2 at 37°C. After two weeks, cells were washed with phosphate-buffered saline (PBS) and fixed with 4% paraformaldehyde for 20 minutes.

Cells were stained with crystal violet. Colonies containing at least 50 cells were counted under a microscope.

CircRNA/miRNA Interaction and Differential genes Analyses

The miRanda (http://www.microrna.org/microrna/home.do) and RNAhybrid (https://bibiserv.cebitec.uni-bielefeld.de/rnahybrid/) databases were utilized to identify potential interacting miRNAs and circRNAs. Additionally, the TargetScan website (https://www.targetscan.org/vert_80/) was used to predict possible interactions between miRNAs and the Tp53 gene. Following the overexpression of hsa_circ_0000038, differentially expressed genes were identified through RNA sequencing (RNA-seq) and subsequent bioinformatics analysis.

A functional cluster analysis of these differentially expressed genes was conducted using Metascape (https://metascape.org/).

Statistical analyses

Data were analyzed using SPSS 17.0 for Windows and plotted using GraphPad Prism 9.0. Expression levels of

hsa_circ_0000038 were analyzed using a paired t-test to compare carcinomatous and normal tissues. Clinical and pathological characteristics of hsa_circ_0000038 expression in HCC patients were assessed by a two-sample t-test. Results are presented as mean ± SD. A p-value <0.05 was considered statistically significant.

RESULTS

The expression levels of hsa_circ_0000038 are downregulated in tissues from liver cancer patients and hepatoma cell lines

The circAtlas 3.0 database (https://ngdc.cncb.ac.cn/circatlas/) indicates that hsa_circ_0000038 is expressed at lower levels in hepatocellular carcinoma (HCC) tissues compared to other cancers (Figure 1A). We recruited twenty pairs of HCC patients (n=20) for this study. The expression of hsa_circ_0000038 was significantly downregulated in liver cancer tissues compared to their paired para-cancerous tissues (Figure 1B). We selected p53 wild-type HepG2 cells, p53-deficient Hep3B cells, and hepatic progenitor cells (HepaRG) for further analysis. Expression levels of hsa_circ_0000038 were significantly lower in the hepatocellular carcinoma cells compared to the HepaRG cells (Figure 1C). To confirm the loop-forming property of hsa_circ_0000038, we designed a pair of divergent primers specifically targeting the back-splice junction site. In genomic DNA, convergent primers amplified a 2738 nt band spanning exon 6, exon 7, and an intron, while divergent primers did not produce specific bands. In cDNA, convergent primers amplified a 783 nt band spanning exon 6 and exon 7, while divergent primers amplified a 282 nt band that spanned the back-splice junction site (Figures 1D and E). The circular structure of hsa_circ_0000038 was further confirmed using an RNase R digestion assay. Results showed that hsa_circ_0000038 was more resistant to the RNase R enzyme compared with linear RNAs in HepG2 cells (Figure 1F). Additionally, with increased duration of actinomycin D treatment, the expression of linear RNA decreased, while circRNA levels remained relatively stable (Figure 1G). These findings indicate that hsa_circ_0000038 possesses a closed-loop structure.

Figure 1: Characterization of hsa_circ_0000038 in liver cancer tissues and cells.

(A)The expression levels of hsa_circ_0000038 in Various cancers analysis by circatlas3.0. Boxplot means the relative ratio in expression level. (B)The expression levels of hsa_circ_0000038 in HCC tissues in comparison with matched normal tissues(n=20) were measured using RT-qPCR. (C) RT-qPCR verified the basial levels of hsa_circ_0000038 in HepG2 cells (p53-wild type) and (p53-deficient type) Hep3B cells and hepatic progenitor cells. (D) After PCR with convergent and divergent primer, gel electrophoresis was performed. (E) The genomic loci of the hsa_circ_0000038 gene. Hsa_circ_0000038 is synthesized at the PHACTR4 gene locus containing exons 6 to 7. The back-splice junction of hsa_circ_0000038 was identified by Sanger sequencing. (F) hsa_circ_0000038 was confirmed as a circRNA that is resistant to RNase R treatment compared to the liner RNA. (G) Expression trends of hsa_circ_0000038 and linear RNA in cells treated with 2.5Ug/ml actinomycin D for 24 h. Each experiment was performed at least three times independently. ** p< 0.01, *** p< 0.001.

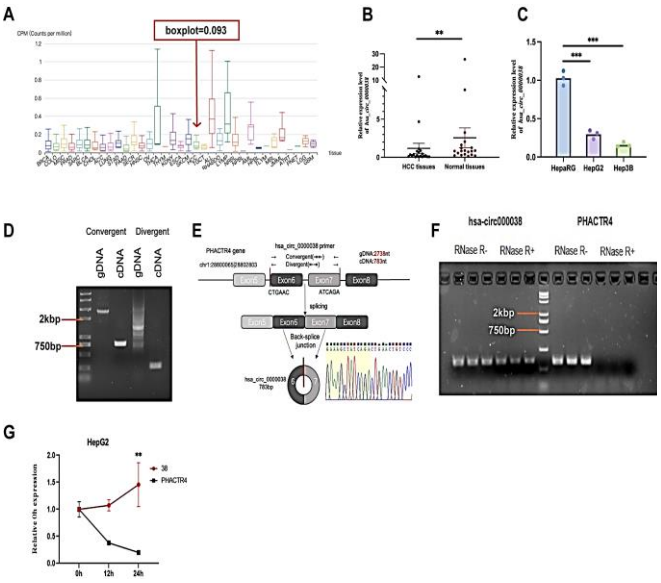

Hsa_circ_0000038 inhibits proliferation, migration, and invasion of cancer cells

After exogenous transfection of the hsa_circ_0000038 plasmid, the expression of hsa_circ_0000038 was elevated in HepG2 and Hep3B cells compared with the circ-NC, whereas after transfection of ASO-circ_0000038, the expression of hsa_circ_0000038(which knocks down hsa_circ_0000038) was specifically silenced compared with ASO-NC (NC control to ASO) (Figure 2A). At the same time, overexpression or silencing of hsa_circ_0000038 failed to upregulate or knock down the expression of the host gene PHACTR4. In HepG2 and Hep3B cells, The CP6 system detected that the upregulation of hsa_circ_0000038 resulted in a decrease in cell proliferation, as indicated by lower values within 96 hours, compared with the circ-NC group (Figure 2B). Transwell assays were used to assess cell migration and invasion. In comparison to ASO-NC treatment, the number of migrating and invaded cells increased following the administration of ASO-circ_0000038 in HepG2 cells.

Conversely, the overexpression of hsa_circ_0000038 decreased the number of migrating and invading cells compared with the circ-NC-transfected group in HepG2 cells (Figure 2C and 2D). In the cell cycle assays, the overexpression of hsa_circ_0000038 in HepG2 cells led to an increase in the number of cells transitioning from S and G2/M phases to G0/G1 phases, compared with the circ-NC-transfected group. When ASO-circ_0000038 was transfected, it led to a higher transformation of cells from G0/G1 phases to S and G2/M phases (Figure 2E and 2F). The behaviour of the cells was observed by colony formation assay. Cell density and cell clonality was significantly higher in HepG2 cells transfected with hsa_circ_0000038 than in HepG2 cells transfected with circ-NC (Figure 2G). While the Hep3B cells showed that cell proliferation was inhibited after overexpression of hsa_circ_0000038. There was no significant difference in cell clonality and cell cycle after overexpression and downregulation of hsa_circ_0000038.

Hsa_circ_0000038 acts as a sponge for miR-92a-2-5p and Tp53 is a target gene of miR-92a-2-5p

Transcriptome analysis revealed that differentially expressed genes were significantly enriched in the p53 transcriptional regulation pathway (R-HAS-3700989) following the overexpression of hsa_circ_0000038 (Figure 3A). Bioinformatics predictions indicated that hsa_circ_0000038 contains two binding sites for miR-92a-2-5p, while miR-92a-2-5p has one binding site on Tp53. Overexpression of hsa_circ_0000038 in HepG2 and Hep3B cells resulted in decreased levels of miR-92a-2-5p. Conversely, silencing hsa_circ_0000038 through ASO transfection led to increased expression of miR-92a-2-5p (Figure 3B). Notably, miR-92a-2-5p was found to be upregulated in HCC tumor tissues compared to adjacent paraneoplastic tissues (Figure 3C). To investigate the binding sites further, two mutants of hsa_circ_0000038, Mut part1-circ_0000038 and Mut part2-circ_0000038, were created by mutating the wild-type hsa_circ_0000038 (Figure 3D). HEK-293T cells were first transfected with either wild-type or mutant hsa_circ_0000038 and subsequently transfected with miR-92a-2-5p six hours later. Results from the dual-luciferase reporter assay indicated that cells transfected with wild-type hsa_circ_0000038 exhibited significantly lower fluorescence activity compared to those transfected with the mutant hsa_circ_0000038, attributed to the overexpression of miR-92a-2-5p (Figure 3E). In RNA immunoprecipitation (RIP) assays, we observed that circRNAs were preferentially enriched in miRNA ribonucleoprotein complexes containing AGO2, compared to control IgG (Figure 3F). These findings suggest that hsa_circ_0000038 can regulate miR-92a-2-5p through target binding in HCC.

Figure 2: hsa_circ_0000038 hampered cell proliferation and changed the ability of migration, invasion and the polarization of cell cycle in vitro.

(A)Verification of hsa_circ_0000038 knockdown or overexpression by RT-qPCR analysis. (B)HepG2(Wild type) and Hep3B (p53- type) cells were transfected with hsa_circ_0000038 or knock downed by ASO. Cell growth was measured with a cell proliferation assay. (C)hsa_circ_0000038 inhibited the migration ability in HepG2(Wild type) cells. ASO could improve the migration in HepG2 cells. (D) hsa_circ_0000038 inhibited the invasion in HepG2 cells. (E, F) hsa_circ_0000038 stagnated the cell cycle in the G1/G0 phase in HepG2 (Wild type), but pushed the cell cycle toward the G2/M phase in Hep3B. ASO has no significant difference in cell cycle with AsoNC groups in Hep3B cells. (G) hsa_circ_0000038 could promote the cell density and clonality in HepG2 cells. In Hep3B, there were no difference among groups. *p<0.05, ** p< 0.01, *** p< 0.001.

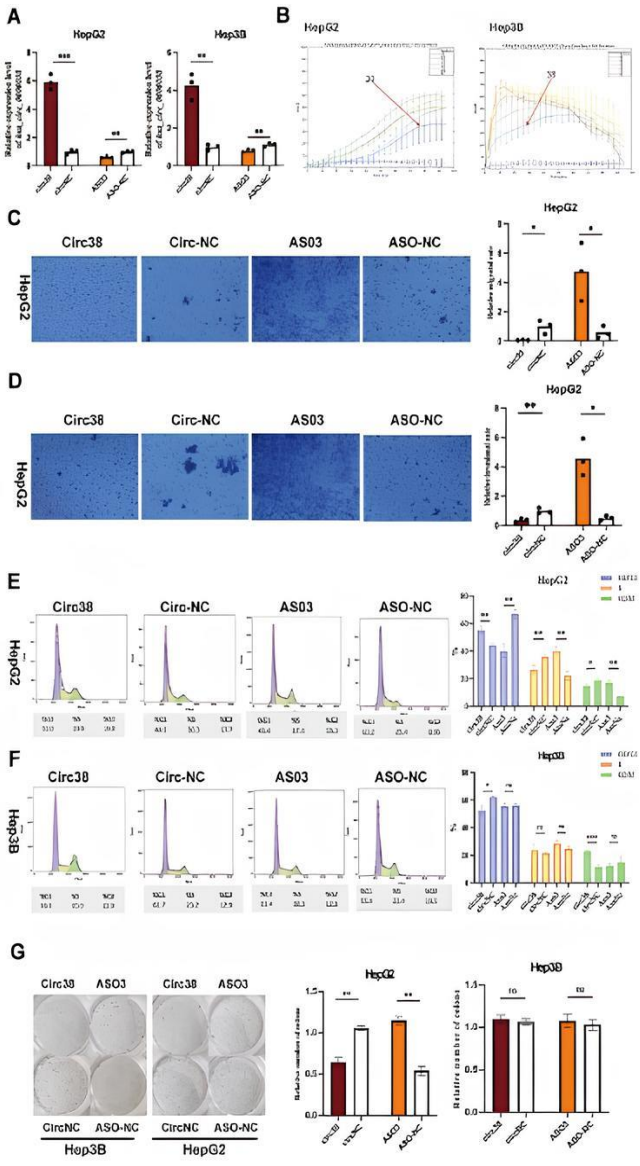

Additionally, both wild-type and mutant Tp53 3'UTRs were constructed (Figure 3G) and analyzed after co-transfection with miR-92a-2-5p in HEK-293T cells. Luciferase activity was significantly reduced in cells transfected with the wild-type Tp53 3'UTR (Figure 3H). Furthermore, the RIP assay confirmed that miR-92a-2-5p was preferentially enriched in mRNA ribonucleoprotein complexes containing AGO2 compared to control IgG (Figure 3I). This evidence supports the notion that Tp53 is a direct functional target gene of miR-92a-2-5p in HCC.

Figure 3: Hsa_circRNA_0000038 functions as a sponge for miR-92a-2-5p, Tp53 was a target gene of miR-92a-2-5p.

(A) Transcriptome analysis also suggested that the downstream pathway may be the p53 pathway. (B) After transfection of hsa_circRNA_0000038, the level of miR-92a-2-5p had been downregulated; when transfecting ASO, the level of miR-92a-2-5p had been upregulated. (C) miR-92a-2-5p has high expression level in 20 paired human HCC compared with adjacent normal liver tissues. (D)This figure showed that miR-92a-2-5p and hsa_circRNA_0000038 could be predicted to directly bind to two different sites, then we compete the design of site variation at the two sites for plasmid synthesis. compared to cells transfected with mut1-hsa_circ_0000038, cells transfected with part1-circ_0000038 cells had significantly lower fluorophore activity because of miR-92a-2-5p overexpression. (E)Dual luciferase reporter assays demonstrated that miR-92a-2-5p is a direct target of hsa_circ_0000038. (F)AGO2 confirmed miR-92a-2-5p and hsa_circRNA_0000038 have direct interaction relationship. (G) Potential binding sites of Tp53 gene and miR-92a-2-5p on the website of Tragetscan. The potential binding site information of miR-92a-2-5p and Tp53 3'UTR is shown in the figure. (H) Dual luciferase reporter assays demonstrated that miR-92a-2-5p is a direct target of Tp53. (I) AGO2 confirmed miR-92a-2-5p and Tp53 have direct interaction relationship. * p< 0.05, ** p<0.01.

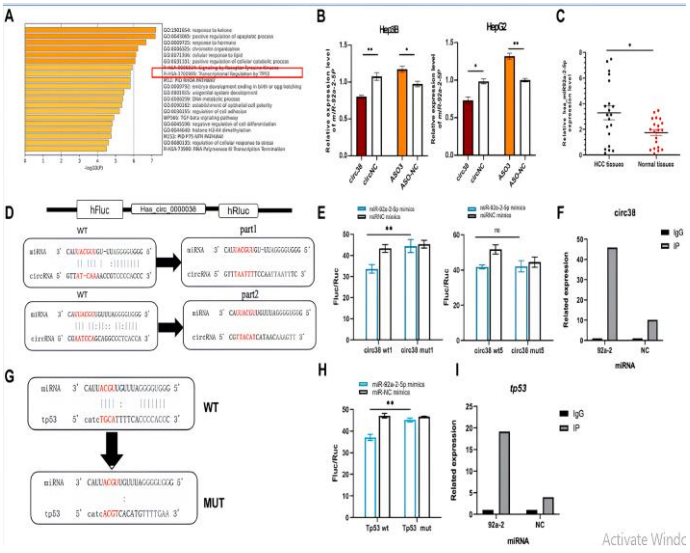

Hsa_circ_0000038 regulate cell signal pathway through miR-92a-2-5p in liver cancer cell lines

We aimed to determine whether Tp53 is a downstream target of the hsa_circ_0000038/miR-92a-2-5p axis. First, western blot analysis revealed that the upregulation of hsa_circ_0000038 resulted in increased levels of p53, p21, p27s compared to the control group (Figure 4A). Moreover, overexpression of miR-92a-2-5p counteracted the expression of p53, p21, and p27 proteins (Figure 4B). This indicates that hsa_circ_0000038 regulates these proteins within the cell signaling pathway. In addition, we conducted the rescuer experiment. Transfection of miR-92a-2-5p mimics partly counteracted the miR-92a-2-5p downregulation induced by the overexpression of hsa_circ_0000038 in HepG2 cells (Figure 4C).

Figure 4: Hsa_circ_0000038 regulate cell signal pathway through miR-92a-2-5p.

(A)The protein levels were measured by WB assays. The expressions of p53/p21, p27 were detected by Western blot in HepG2 cells and Hep3B cells respectively transfected with hsa_circ_0000038 and ASO. (B) After co-transfection of hsa_circ_0000038(ASO) and miR-92a-2-5p mimics(inhibitor), the cell signal pathway protein have been detected to investigate the interaction between hsa_circ_0000038 and miR-92a-2-5p in translation levels. These figures indicated co-transfection of miR-92a-2-5p mimics and hsa_circ_0000038 partly counteracted (C) the miR-92a-2-5p downregulation induced by the overexpression of hsa_circ_0000038. and (D) cell proliferation ability inhibition and (E) cell invasion capacity inhibition. (F, G) The CCK-8 assay, and invasion results showed that the p53 inhibitor pifithrin-α partially reversed the down-regulation of cell proliferation mediated by the hsa_circ_0000038. *p<0.05, ** p< 0.01, *** p< 0.001

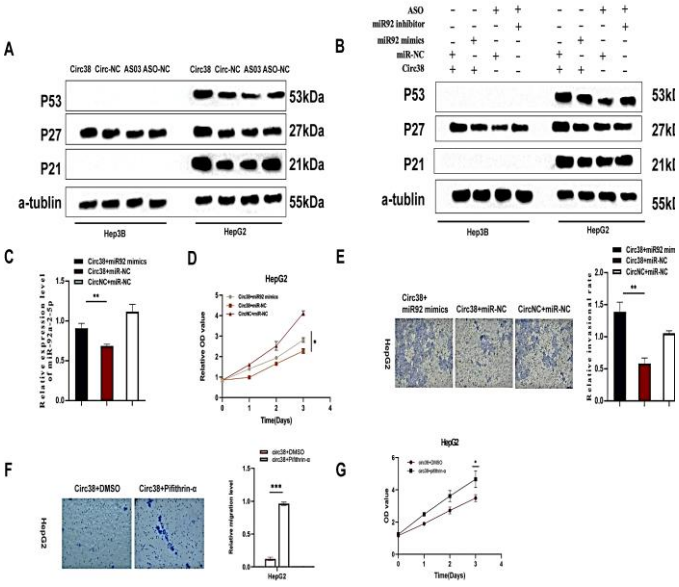

HepG2 cell proliferation was inhibited by hsa_circ_0000038, but the effect was lessened by the application of miR-92a-2-5p mimics (Figure 4D). The suppression of Transwell invasion, was also partly counteracted in oe-hsa_circ_0000038. (Figure 4E) Next, CCK-8 assay results demonstrated that the p53 inhibitor pifithrin-α partially reversed the downregulation of cell proliferation caused by hsa_circ_0000038 (Figure 4F). Similar outcomes were observed in the invasion assay (Figure 4G). Changes in miR-92a-2-5p levels correlated with the expression of hsa_circ_0000038, further supporting our hypothesis. In summary, hsa_circ_0000038 regulates p53/p21 protein expression by binding to the 3'UTR of Tp53 mRNA via miR-92a-2-5p.

DISCUSSION

CircRNAs are increasingly recognized as novel and unique genetic regulators or biomarkers in the field of cancer research. Dysregulation of their expression or splicing can significantly impact neoplasia development Goodall et al. (2021), Bradley et al. (2023). They are highly stable and detectable in plasma samples and have been shown to regulate tumor progression by influencing tumor cell cycle, apoptosis, autophagy, immune surveillance effects, vascular regenerative capacity, and cellular energy Kristensen et al. (2022). In rapidly proliferating tumor cells, circRNAs may not be directly involved in cancer progression, but their expression levels can serve as robust prognostic indicators Dahl et al. (2022). The predominant mechanism involves circRNAs effectively modulating the expression and translation of downstream target genes by binding and sequestering miRNAs, thus acting as molecular sponges Ebert et al. (2010), Hansen et al. (2013).

In our study, we used RT-qPCR to confirm that hsa_circ_0000038 was expressed at a low level in HCC tissues as well as in HCC cell lines. Through functional experiments, we found that over-expression of hsa_circ_0000038 significantly decreased cell viability and proliferation while si-circ_0000038 increased cell viability and proliferation. These results demonstrate that hsa_circ_0000038 serves as a cancer suppressor in HCC progression. miR-92a-2-5p has been identified as a target of hsa_circ_0000038. Our findings demonstrate a negative correlation between hsa_circ_0000038 and miR-92a-2-5p. Rescue experiments indicated that the reduction in cell proliferation and invasion caused by hsa_circ_0000038 can be reversed by miR-92a-2-5p mimics. Additionally, dual-luciferase reporter assays and RNA immunoprecipitation confirmed the presence of direct binding sites. These results suggest that hsa_circ_0000038 functions as an anti-oncogene by targeting miR-92a-2-5p.

To explore the role of p53 in the tumor-suppressing effects of hsa_circ_0000038, we selected two different cell lines. The Tp53 gene is recognized as a key regulator of various tumorigenic processes Qiang et al. (2020). Recent studies have examined the relationship between circRNA and p53 in multiple cancers Li et al. (2020), Lu et al. (2020), Liu et al. (2022). Notably, our observations revealed differing trends in protein expression changes between Hep3B and HepG2 cells following manipulation of hsa_circ_0000038 levels.

p21, a member of the Cip family, serves as a cyclin-dependent kinase inhibitor and is regulated downstream of p53 El-Deiry et al. (1993), Deng et al. (1995). The p21 promoter contains two strong p53-responsive elements; therefore, when p53 accumulates, p21 mRNA levels rise sharply. Elevated p21 levels trigger cell cycle arrest in the G1 and G2 phases Deng et al. (1995), Warfel et al. (2013). In our study, we observed a significant upregulation of p21 in HepG2 cells after modifying hsa_circ_0000038 levels, leading to cell cycle arrest and inhibition of clonogenicity. Conversely, due to the absence of p53 expression, Hep3B cells could not exert the regulatory effects of p21 on cell cycle progression and clonogenicity following hsa_circ_0000038 intervention. These results indicate that hsa_circ_0000038 inhibits HCC progression primarily through the p53/p21 pathway.

Consequently, hsa_circ_0000038 functions as a p53 activator and may serve as a novel diagnostic target, potentially benefiting HCC patients in the future. The roles of the p53 gene encompass the regulation of the cell cycle, apoptosis, senescence, DNA repair, metabolism, and metastasis Choudhary et al. (2023). These findings underscore a significant anti-cancer effect that could inform cancer treatment strategies and targeted drug development. However, several limitations exist. First, a larger sample size is required to validate its diagnostic efficacy. Second, we did not assess the prognostic significance of elevated hsa_circ_0000038 levels in HCC. Third, in vivo evidence will be necessary to further support our conclusions.

CONCLUSION

Analysis of HCC samples and cell lines revealed decreased expression levels of hsa_circ_0000038. Functional assays demonstrated that hsa_circ_0000038 impedes cell proliferation, clonogenic formation, migration, invasion, and cell cycle progression in HepG2 cells. Furthermore, miR-92a-2-5p was identified as a direct target of hsa_circ_0000038, while p53 was found to be a direct target of hsa_circ_0000038, while p53 was found to be a direct target of miR-92a-2-5p.

Western blot analysis showed that hsa_circ_0000038 upregulates p53, p21, and p27 proteins. These results indicate that hsa_circ_0000038 inhibits HCC progression primarily by targeting the p53/p21 pathway through the sponge effect on miR-92a-2-5p. This study elucidates the specific role of hsa_circ_0000038 in HCC and details its cell cycle signaling pathways, thereby highlighting its biological significance.

DECLARATIONS

Funding

This work was supported by grants from National Natural Science Foundation of China (NO.8206080407) and Yunnan Provincial Department of Science and Technology-Kunming Medical University Basic Research Joint Special Project (202101AY070001-283). Young and middle-aged academic and technical leaders reserve talents in Yunnan Province (202205AC160023); Special fund of the Yunnan University "double first-class" construction.

Competing interest

The authors declare no competing financial interests.

Authors' contributions

J. W. and T. C. Z. designed the study; S. H. Z. and M. T. L., Z. Y. Z. performed the experimental procedures; S. H. Z. and T. C. Z performed the data analysis; S. H. Z. drafted the manuscript. T.C.Z and M. T. L. Revised manuscript. Q.F and R.C.Z collected the clinical samples; all authors contributed to and have approved the final manuscript.

Ethics approval and consent to participate

Details are in supplement material ethics review form.

Data Availability

All datasets generated during the study are described in the Supplementary Data section and/or available from the corresponding author upon reasonable request.

REFERENCES

1. Sung H, Ferlay J, Siegel RL, et al. 2021. Global Cancer Statistics 2020: GLOBOCAN Estimates of Incidence and Mortality Worldwide for 36 Cancers in 185 Countries. CA Cancer J Clin. 71(3):209-49.

2. Llovet JM, Kelley RK, Villanueva A, et al. 2021. Hepatocellular carcinoma. Nat Rev Dis Primers. 7(1):6.

3. Ayuso C, Rimola J, Vilana R, et al. 2018. Diagnosis and staging of hepatocellular carcinoma (HCC): current guidelines. Eur J Radiol. 101:72-81.

4. Yang JD, Hainaut P, Gores GJ, et al. 2019. A global view of hepatocellular carcinoma: trends, risk, prevention and management. Nat Rev Gastroenterol Hepatol. 16(10):589-04.

5. Sugawara Y, Hibi T. 2021. Surgical treatment of hepatocellular carcinoma. Biosci Trends. 15(3):138-41.

6. Reig M, Forner A, Rimola J, et al. 2022. BCLC strategy for prognosis prediction and treatment recommendation: The 2022 update. J Hepatol. 76(3):681-93.

7. Singal AG, Kudo M, Bruix J. 2023. Breakthroughs in Hepatocellular Carcinoma Therapies. Clin Gastroenterol Hepatol. 21(8):2135-49.

8. Huang G, Liang M, Liu H, et al. 2020. CircRNA hsa_circRNA_104348 promotes hepatocellular carcinoma progression through modulating miR-187-3p/RTKN2 axis and activating Wnt/beta-catenin pathway. Cell Death Dis. 11(12):1065.

9. Yao T, Chen Q, Fu L, et al. 2017. Circular RNAs: Biogenesis, properties, roles, and their relationships with liver diseases. Hepatol Res. 47(6):497-04.

10. Mohammadi D, Zafari Y, Estaki Z, et al. 2022. Evaluation of plasma circ_0006282 as a novel diagnostic biomarker in colorectal cancer. J Clin Lab Anal. 36(1): e24147.

11. Xiong DD, Dang YW, Lin P, et al. 2018. A circRNA-miRNA-mRNA network identification for exploring underlying pathogenesis and therapy strategy of hepatocellular carcinoma. J Transl Med. 16(1):220.

12. Wang L, Wu J, Xie C. 2017. miR-92a promotes hepatocellular carcinoma cells proliferation and invasion by FOXA2 targeting. Iran J Basic Med Sci. 20(7):783-90.

13. Gong Y, Mao J, Wu D, et al. 2018. Circ-ZEB1.33 promotes the proliferation of human HCC by sponging miR-200a-3p and upregulating CDK6. Cancer Cell Int. 18:116.

14. Ueda H, Ullrich SJ, Gangemi JD, et al. 1995. Functional inactivation but not structural mutation of p53 causes liver cancer. Nat Genet. 9(1):41-7.

15. Muller M, Meyer M, Schilling T, et al. 2006. Testing for anti-p53 antibodies increases the diagnostic sensitivity of conventional tumor markers. Int J Oncol. 29(4):973-80.

16. Lieschke E, Wang Z, Kelly GL, et al. 2019. Discussion of some 'knowns' and some 'unknowns' about the tumour suppressor p53. J Mol Cell Biol. 11(3):212-23.

17. Fischer JW, Leung AKL. 2017. CircRNAs: a regulator of cellular stress. Crit Rev Biochem Mol Biol. 52(2):220-33.

18. Du WW, Fang L, Yang W, et al. 2017. Induction of tumor apoptosis through a circular RNA enhancing Foxo3 activity. Cell Death Differ. 24(2):357-70.

19. Goodall GJ, Wickramasinghe VO. 2021. RNA in cancer. Nat Rev Cancer. 21(1):22-36.

20. Bradley RK, Anczukow O. 2023. RNA splicing dysregulation and the hallmarks of cancer. Nat Rev Cancer. 23(3):135-55.

21. Kristensen LS, Jakobsen T, Hager H, et al. 2022. The emerging roles of circRNAs in cancer and oncology. Nat Rev Clin Oncol. 19(3):188-06.

22. Dahl M, Husby S, Eskelund CW, et al. 2022. Expression patterns and prognostic potential of circular RNAs in mantle cell lymphoma: a study of younger patients from the MCL2 and MCL3 clinical trials. Leukemia. 36(1):177-88.

23. Ebert MS, Sharp PA. 2010. Emerging roles for natural microRNA sponges. Curr Biol. 20(19): R858-61.

24. Hansen TB, Jensen TI, Clausen BH, et al. 2013. Natural RNA circles function as efficient microRNA sponges. Nature. 495(7441):384-8.

25. Qiang J, He J, Tao YF, et al. 2020. Hypoxia-induced miR-92a regulates p53 signaling pathway and apoptosis by targeting calcium-sensing receptor in genetically improved farmed tilapia (Oreochromis niloticus). PLoS One. 15(11): e0238897.

26. Li X, Lin S, Mo Z, et al. 2020. CircRNA_100395 inhibits cell proliferation and metastasis in ovarian cancer via regulating miR-1228/p53/epithelial-mesenchymal transition (EMT) axis. J Cancer. 11(3):599-09.

27. Lu C, Jiang W, Hui B, et al. 2020. The circ_0021977/miR-10b-5p/P21 and P53 regulatory axis suppresses proliferation, migration, and invasion in colorectal cancer. J Cell Physiol. 235(3):2273-85.

28. Liu J, Qiao X, Liu J, et al. 2022. Identification of circ_0089153/miR-608/EGFR p53 axis in ameloblastoma via MAPK signaling pathway. Oral Dis. 28(3):756-70.

29. El-Deiry WS, Tokino T, Velculescu VE, et al. 1993. WAF1, a potential mediator of p53 tumor suppression. Cell. 75(4):817-25.

30. Deng C, Zhang P, Harper JW, et al. 1995. Mice lacking p21CIP1/WAF1 undergo normal development, but are defective in G1 checkpoint control. Cell. 82(4):675-84.

31. Warfel NA, El-Deiry WS. 2013. p21WAF1 and tumourigenesis: 20 years after. Curr Opin Oncol. 25(1):52-8.

32. Choudhary HB, Mandlik SK, Mandlik DS. 2023. Role of p53 suppression in the pathogenesis of hepatocellular carcinoma. World J Gastrointest Pathophysiol. 14(3):46-70.

